

# CYCLONE GLOBAL NAVIGATION SATELLITE SYSTEM (CYGNSS)



<b>Algorithm Theoretical Basis Document Level 1A DDM Calibration</b>	<b>UM Doc. No.</b>	<b>148-0136</b>
	<b>SwRI Doc. No.</b>	<b>N/A</b>
	<b>Revision</b>	<b>2</b>
	<b>Date</b>	<b>20 Aug 2018</b>
	<b>Contract</b>	<b>NNL13AQ00C</b>

Algorithm Theoretical Basis Documents (ATBDs) provide the physical and mathematical descriptions of the algorithms used in the generation of science data products. The ATBDs include a description of variance and uncertainty estimates and considerations of calibration and validation, exception control and diagnostics. Internal and external data flows are also described.



# CYCLONE GLOBAL NAVIGATION SATELLITE SYSTEM (CYGNSS)

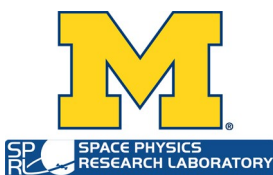


<b>Algorithm Theoretical Basis Document Level 1A DDM Calibration</b>	<b>UM Doc. No.</b>	<b>148-0136</b>
	<b>SwRI Doc. No.</b>	<b>N/A</b>
	<b>Revision</b>	<b>2</b>
	<b>Date</b>	<b>20 Aug 2018</b>
	<b>Contract</b>	<b>NNL13AQ00C</b>

Prepared by:

\_\_\_\_\_  
Scott Gleason, Southwest Research Institute

Date: \_\_\_\_\_



Approved by: \_\_\_\_\_ Date: \_\_\_\_\_  
 Chris Ruf, CYGNSS Principal Investigator

Approved by: \_\_\_\_\_ Date: \_\_\_\_\_  
 Jillian Redfern, CYGNSS MOC Manager

Approved by: \_\_\_\_\_ Date: \_\_\_\_\_  
 Tim Butler, CYGNSS SOC Manager

Released by: \_\_\_\_\_ Date: \_\_\_\_\_  
 Darren McKague, CYGNSS Project Manager

### REVISION NOTICE

Document Revision History		
Revision	Date	Changes
PRE-RELEASE DRAFT	17 June 2013	n/a
INITIAL RELEASE	14 January 2014	Add explicit algorithms for use of internal black body target and estimation of receiver noise temperature. Add detailed error analysis.
Rev 1	19 December 2014	Same basic approach but greater detail and examples provided of algorithm implementation.
Rev 2	20 August 2018	Inclusion of all modifications made to the Level 1A algorithms based on observed on-orbit performance between March 2017 and August 2018.





## I. INSTRUMENT LEVEL 0 MEASUREMENTS

This is a portion of the overall Level 1 Calibration Algorithm Theoretical Basis Document (ATBD) describing the Level 1a calibration and error analysis.

Individual bins of the DDM generated by the Delay Doppler Mapping Instrument (DDMI) are measured in raw, uncalibrated units referred to as "counts". These counts are linearly related to the total signal power processed by the DDMI. In addition to the ocean surface scattered Global Positioning System (GPS) signal, the total signal includes contributions from the thermal emission by the Earth and by the DDMI itself. The power in the total signal is the product of all the input signals, multiplied by the gain of the DDMI receiver. Level 1a calibration converts each bin in the DDM from raw counts to units of watts. A flowchart of the L1a calibration procedure is shown in Figure 1.

1) *Calibration Intervals*: The black body calibration will be performed every 60 seconds on-orbit for each nadir science antenna. The routine calibration will be performed at 1Hz on all DDM's output by the DDMI (4 per second).

### A. Level 0 Delay Doppler Map

The DDM values output from the CYGNSS science instrument will be sent to the CYGNSS spacecraft as arbitrary counts. The count values will be a result of the signal traveling through the various stages of the instrument, which will add a gain to the received power levels. The value of the pixels in the DDM in arbitrary counts can be linked to the arriving signal power in Watts such that,

$$C = G(P_a + P_r + P_g) \quad (1)$$

where,

$C$  are the DDM values in counts output from the instrument at each delay/Doppler bin.

$P_a$  is the thermal noise power received by the antenna in watts.

$P_r$  is the thermal noise power generated by the instrument in watts.

$P_g$  is the scattered signal power received by the instrument in watts.

$G$  is the total instrument gain applied to the incoming signal and noise in counts per watt.

The terms,  $C$  and  $P_g$  are functions of delay and Doppler while  $P_a$  and  $P_r$  are assumed to be independent of the delay Doppler bin in the DDM. Every DDM includes a number of delay bins where signal power is not present and an individual DDM noise floor level can be estimated. These bins physically represents delays above the ocean surface. These delay and Doppler bins provide an estimate of the DDM noise power, expressed in counts as,

$$C_N = G(P_a + P_r) \quad (2)$$

Assuming  $P_a$  and  $P_r$  are independent of delay and Doppler, the DDM samples above the ocean surface can be used to estimate the noise only contribution to the raw counts expressed in Equation 1.

### B. Noise Power Expressions

The input antenna noise can be generically expressed as,

$$P_a = kT_a B_W \quad (3)$$

where  $T_a$  is the top of the atmosphere brightness temperature integrated over the receive antenna pattern,  $k$  is Boltzmann's constant and  $B_W = \frac{1}{T_i} = 1000Hz$  is the signal bandwidth. The bandwidth of the GPS signal at the antenna is determined by the coherent integration processing interval, which is  $T_i = 1$  ms.

When the instrument input is switched to the calibration load, the input antenna noise becomes,

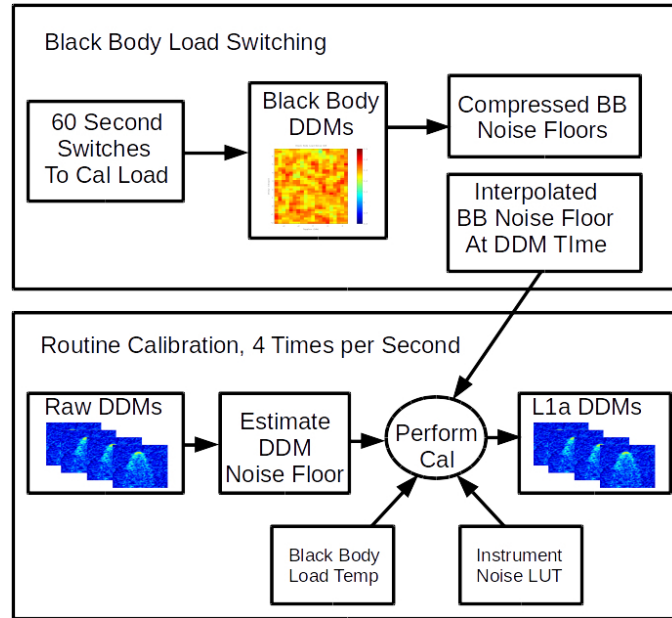


Fig. 1. Overview of CYGNSS Level 1a Calibration. The switches to the calibration load on each of the nadir antennas is performed every 60 seconds to obtain an estimate of the instrument only noise counts  $C_B$ . This in combination with the estimated DDM noise floor  $C_N$ , black body load physical temperature  $T_I$  and pre-launch characterized instrument noise power  $P_r$  are used to generate the calibrated L1a DDMs.

$$P_B = kT_I B_W \quad (4)$$

where,  $P_B$  and  $T_I$  are the noise power and effective temperature of the instrument black body load source. The black body load resistor lies on thermal continuous LNA main board where temperature sensor is located, thus BB load temperature and LNA portion of the instrument are assumed to be nearly equivalent.  $T_I$  refers to the physical temperature of the Instrument LNA and black body load resistor in this analysis.

The instrument thermal noise power can be expressed as a function of the instrument noise figure,

$$P_r = kT_r B_W = k[(NF - 1)290]B_W \quad (5)$$

where,  $P_r$  and  $T_r$  are the instrument noise power and temperature. The receiver noise figure  $NF$  is directly related to the instrument noise temperature. The noise figure versus temperature profile was characterized pre-launch for all instrument LNAs, providing an accurate estimate of the instrument noise figure as a function of temperature, from which the instrument noise power can be calculated using Equation 5.

### C. Instrument Calibration Measurements

The instrument noise power will be initially calculated using gain and noise figure temperature profiles generated pre-launch for both instrument LNAs on each satellite. Using these tables the instrument noise power can be estimated directly from the LNA temperature  $T_r$  and Equation 5.

Subsequently, the expression for the DDM noise counts when the instrument is switched to the black body calibration load can be calculated as,

$$C_B = G(P_B + P_r) \quad (6)$$

where  $P_B$  is the black body noise power and  $P_r$  is the instrument power.  $P_B$  can be calculated using Equation 4 and  $P_r$  is calculated using pre-launch look up tables and Equation 5.



#### D. Instrument Noise Power Estimation Using Look Up Table

It will be necessary to estimate the instrument noise power at every measurement due to LNA temperature fluctuations. This will be done using a look up table derived from measured characteristics of the LNA gain and noise figure as a function of temperature. Thermal testing of the LNA noise figure performance as a function of temperature for all 27 CYGNSS LNAs (1 zenith and two nadir per spacecraft) was performed over several thermal cycles to generate a best linear fit function which is used to estimate the noise figure as a function of temperature on-orbit.

The mean standard deviation of the noise figure across the range of temperatures is 0.027 dB. The maximum slope is 0.0088 dB/DegC, which when multiplied by the temperature uncertainty results in an estimated error in the instrument noise figure of 0.018 dB due to temperature uncertainty. The total noise figure error is taken as the RSS of the standard deviation of the measurements and the temperature error, which is 0.032 dB.

The temperature of the LNA is read at 1Hz and the value of the instrument noise figure is retrieved from a LUT generated from pre-launch testing. The LUT is then updated on orbit using instrument noise floor estimates performed at sufficient intervals to track slow changes in the LNA performance. The instrument noise figure from the LUT is related to the instrument noise power using Equation 5.

#### E. Updating Instrument LUTs On-Orbit

The strategy for updating the pre-launch  $NF$  versus temperature LUTs has changed from the initial L1a ATBD. During its first year on orbit it was not possible to identify Earth surface areas which produced consistent and predicible noise levels, from which a stable open ocean noise value could be reliably used. This is believed to be due largely to the fact that the CYGNSS science antennas are both canted toward the spacecraft along track and have a relatively large main lobe with significant gain. This large look area to both the port and starboard sides of the spacecraft enabled surface noise from very large areas over the Earth surface to enter the main antenna beams. This made it very difficult to isolate even the most remote regions of open ocean and obtain a reliable open ocean noise reference.

Therefore, an alternative method is being designed for the monitoring and updating of the  $NF$  calibration tables on orbit. Fortunately, the CYGNSS LNAs are proving to be remarkably stable, even after more than 1-year on orbit. A number of techniques using the full set of existing on-orbit data are being used to quantify the changing instrument noise figure as the instrument ages on-orbit.

The alternative algorithm starts with the basic equation for the per-DDM noise floor (Equation 2) and the equation for the black body load noise counts (Equation 6). As the instrument noise  $P_r$  and instrument gain  $G$  will both change as the LNAs age, its necessary to re-arrange these two equations to arrive at an expression for  $P_r$  that does not depend on  $G$ . By re-arranging Equations 2 and 6 we arrive at an expression for the instrument noise power,

$$P_r(T_I) = \frac{C_N(T_I)P_B(T_I) - C_B(T_I)P_a}{C_N(T_I) - C_B(T_I)} \quad (7)$$

Were several of the above variables are represented as functions of the LNA instrument physical temperature  $T_I$ . As the daily measurement distribution for each CYGNSS satellite is roughly repeatable over longer time intervals, the mean noise floor and black body load versus physical temperature dependence for each LNA will exhibit reliable statistical behavior over monthly intervals, from which changes in  $P_r$  and  $T_r$  can be estimated.

By re-arranging Equation 5 the instrument noise power,  $T_r$ , and noise figure,  $NF$ , can then be estimated from the on-board estimated instrument noise power as a function of physical LNA temperature as,

$$T_r(T_I) = \frac{P_r(T_I)}{kB_W} \quad (8)$$

$$NF(T_r) = \frac{P_r(T_I)}{k290B_W} + 1 \quad (9)$$

Estimates of the instrument noise power as a function of the physical noise temperature,  $P_r(T_I)$ , with the instrument noise power equivalent temperature,  $T_r$  derived from Equation 5 can then be fit with a linear regression technique to quantify the changing relationship between the physical and noise power temperatures from month to month on orbit. Subsequently, the LUT entry for a given LNA at a given temperature can then be updated over the orbit life of the LNA and correct for changes in the LNA noise figure at one month intervals as the instrument ages.



## II. ROUTINE CALIBRATION OF SIGNAL POWER

The generic instrument DDM in counts is expressed in Equation 1, which includes the received signal power,  $P_g$ . These DDMs will be generated by the instrument every second and will be corrected by the estimated noise floor expressed in Equation 2 and calculated using noise only bins in the DDM, such that we are left with a signal only DDM,

$$C_g = C - C_N = GP_g \quad (10)$$

Subsequently the instrument gain at the collection time of the DDM can be calculated using the current estimate of the LNA physical temperature,  $T_I$ , from which we estimate the instrument noise power,  $P_r$ . This is achieved by re-arranging Equation 10 into an expression of the instrument gain, and setting this equal to the instrument gain expression obtained from the black body load calibration DDM from Equation 6,

$$G = \frac{C - C_N}{P_g} = \frac{C_B}{P_B + P_r} \quad (11)$$

where,  $C_B$  is the best estimate mean counts of the black body load DDM at the time of the measurement being calibrated. The black body load counts are linearly interpolated to the second of the measurement using black body DDMs before and after the DDM being calibrated.

$P_B$  is the estimated black body load noise power estimated using the last LNA instrument thermistor temperature reading  $T_I$  near the load itself in the LNA, and Equation 4. Taken within a second of the DDM being calibrated.

$P_r$  is the estimate of the instrument noise power, estimated from the noise figure vs physical temperature ( $T_I$ ) look up table generated pre-launch for this specific LNA.

### A. Generating the Level 1a Data Product

The routine calibration assumes that the Gain,  $G$ , antenna noise temperature  $T_a$ , and the instrument noise power  $P_r$ , remain constant over the combined collection interval for Equation 1 (DDM to be calibrated) and Equation 2 (Noise floor estimate for the DDM being calibrated). The black body noise counts used in Equation 6 is linearly interpolated from black body DDMs before and after the calibration DDM to the measurement time. By substituting Equation 11 into Equation 10 and solving for the signal power term,  $P_g$  we arrive at the final Level 1a calibration,

$$P_g = \frac{(C - C_N)(P_B + P_r)}{C_B} \quad (12)$$

Equation 12 is applied to all pixels of the compressed Level 0 DDMs (11 Doppler bins x 17 delay bins) four times per second for each instrument measurement channel.

### B. Consideration of Time and Temperature Dependencies

All of the terms in Equation 12 are collected at slightly different times than the actual science measurements themselves, and during these time intervals it is possible that the noise temperatures can vary slightly from the measurement time. Each of the terms in the Level 1a calibration equation is addressed below with regard to this time difference,

- 1)  $C$ . The science measurement is made once per second per channel and provides the reference time for all of the other parameters.
- 2)  $C_N$  The noise measurements for each science DDM are made at delays above the ocean surface, which are only on the order of a handful of microseconds from the time of the science measurement.
- 3)  $P_B$  the blackbody target power is determined from a physical temperature sensor measured at 1 Hz and near enough in time to the 1 Hz science measurements that the physical temperature will not have changed significantly between the thermistor reading and the science measurement.
- 4)  $P_r$  the receiver noise power is derived from a pre-launch generated LUT and will be subject to change over the mission lifetime due to instrument aging effects. This will be corrected by periodically updating the calibration LUTs over the duration of the mission as described above. It is expected that the aging effects to occur on a very slow time scale, on the order of several months.
- 5)  $C_B$  the blackbody target measurement is made within 30 seconds of the science measurement and linearly interpolated to the measurement time using black body measurements before and after the DDM being calibrated. Any changes



in the instrument temperature over up to 30 seconds should be adequately mitigated by this interpolation.

The LUTs used to estimate  $P_r$  will be periodically updated on orbit. The dependence of  $P_r$  on temperature has been initially characterized in pre-launch environmental testing and the baseline flight lookup table was derived from those test data. Once on orbit, monthly observations of the noise floor and black body will be used to validate  $P_r$  using Equation 7. As monthly data is analyzed the lookup tables for each LNA on each satellite will be updated on orbit as required.

### C. Quality Control Flags

The Level 1 data product will include a set of quality control flags designed to indicate to users potential problems with the data. Refer to the CYGNSS Level 1b ATBD for a complete list of quality flags [4].

## III. ERROR ANALYSIS OF THE LEVEL 1A CALIBRATION ALGORITHM

The Level 1a data product consists of observed signal power,  $P_g$  (in Watts) over a range of delay steps and Doppler frequencies. This error analysis concentrates on the uncertainties present in the CYGNSS Level 1a calibration algorithm. Each uncertainty in the Level 1a calibration algorithm will be considered an independent uncorrelated error source. The method for this error analysis is based on that presented in Jansen et. al [1] for a microwave radiometer. The errors in the L1a calibration can be broken into two parts; the estimation of the instrument noise performed during the open ocean calibration sequence,  $P_r$ , and the routine second by second calibration of the science DDM,  $P_g$ .

Equation 12 for the routine calculation of the calibrated signal power is repeated below,

$$P_g = \frac{(C - C_N)(P_B + P_r)}{C_B} \quad (13)$$

The total error in the estimate of the signal power,  $P_g$ , is the root sum square (RSS) of the individual errors contributed by the independent terms of Equation 13, expressed as,

$$\Delta P_g = \left[ \sum_{i=1}^5 E^2(p_i) \right]^{1/2} \quad (14)$$

where the partial derivatives of the individual errors terms can be expressed as,

$$E(p_i) = \left| \frac{\partial P_g}{\partial p_i} \right| \Delta p_i \quad (15)$$

The individual error quantities are defined as:  $p_1 = C$ ,  $p_2 = C_N$ ,  $p_3 = P_B$ ,  $p_4 = P_r$  and  $p_5 = C_B$ . The 1-sigma uncertainties in these quantities are expressed as  $\Delta p_i$ . Using Equation 13 and Equation 15 to evaluate the partial derivative error terms we obtain,

$$E(C) = \frac{P_B + P_r}{C_B} \Delta C \quad (16)$$

$$E(C_N) = \frac{P_B + P_r}{C_B} \Delta C_N \quad (17)$$

$$E(P_B) = \frac{C - C_N}{C_B} \Delta P_B \quad (18)$$

$$E(P_r) = \frac{C - C_N}{C_B} \Delta P_r \quad (19)$$

$$E(C_B) = \frac{(C - C_N)(P_B + P_r)}{C_B^2} \Delta C_B \quad (20)$$

The 1-sigma uncertainties in these quantities are expressed as  $\Delta p_i$ . The L1a 1-sigma uncertainties and the resulting partial derivative error terms are shown in Table I.



**ATBD Level 1A DDM Calibration**

Error Term	Error Magnitude, dB	Comment
	At 10 m/s Reference Wind	
$E(C)$	0.10	Quantization and non-common mode interference
$E(CN)$	0.14	DDM Noise Floor (45 row by 20 pixel average)
$E(PB)$	2 degrees C	Calibration Load Noise Power (from load temperature)
$E(Pr)$	0.14	Instrument Noise Power (from pre-launch LUT uncertainty)
$E(CB)$	0.05	Calibration Load DDM Noise Counts
Total RSS L1a Error	0.13	From Partial Derivatives and MC Simulation

TABLE I  
 ESTIMATES LEVEL 1A 1-SIGMA UNCERTAINTIES, INDIVIDUAL ERROR CONTRIBUTIONS AND ROLLED UP L1A ERROR ESTIMATE.

How each of the 1-sigma error levels in Table I was arrived at is described below.

- 1)  $\Delta C$  is the combination of the quantization error (negligible) and non-common mode contributions to the signal counts. The later can include cross correlations with other GPS satellites which would not effect the signal and noise floors equally and cancel out in the L1a calculation made in Equation 12. Although not possible to accurately quantify exactly the error that may be introduced in the actual data, simulations showed that as a worse case, for certain PRN cross correlations, this error could be up to 0.1 dB.
- 2)  $\Delta CN$  is driven by the number of noise bins averaged during the routine calibration. This method has not changed from the analysis presented in [?]. However, the more conservative high wind speed value of 0.14 dB is used to better bound the error and to account for the possibility for mild RFI levels which would not be detected by the RFI detection algorithm.
- 3)  $\Delta PB$  is determined by the accuracy of the temperature sensor on the black body calibration load.
- 4)  $\Delta Pr$  was calculated from the 1-sigma variation in the pre-launch raw measurements used to generate the instrument noise figure vs temperature look up table.
- 5)  $\Delta CB$  is estimated from the expected error after averaging a full black body calibration DDM (128 rows by 20 columns) every 60 seconds. Includes a small error component due to the propagation to the DDM measurement time between 60 second switches to the calibration load.

REFERENCES

[1] Jansen, M.A., Ruf, C.S. and S.J. Keihm (1995), TOPEX/Poseidon Microwave Radiometer (TMR): II. Antenna Pattern Correction and Brightness Temperature Algorithm, IEEE Trans. Geosci. Remote Sens., Vol. 33, No. 1, pp. 138-146, January 1995.  
 [2] O'Brien, A., Gleason S., Johnson J., and C. Ruf, The End-to-End Simulator for the Cyclone GNSS (CYGNSS) Mission, Submitted to IEEE Transactions on Geoscience and Remote Sensing, Dec 2014.  
 [3] Gleason S., Lowe S. and Zavorotny V. (2009), Remote Sensing Using Bistatic GNSS Reflections, in GNSS Applications and Methods, S. Gleason and D. Gebre-Egziabher (editors), Artech House (Norwood, MA), 2009.  
 [4] CYGNSS Science Team, CYGNSS Level 1b DDM Algorithm Theoretical Basis Document, 2017.